Removal of lead (II) from aqueous solutions by adsorption onto activated carbons prepared from coconut shell

Matteo Caccin[a], Massimo Giorgi[a], Francesca Giacobbo[a], Mirko Da Ros[a], Luigi Besozzi[b], Mario Mariani[a]

[a] *Nuclear Engineering Section, Department of Energy, Politecnico di Milano, via Ponzio 34/3, 20133 Milan, Italy, Tel. +39 0223996300; Fax: +39 0223996309; emails: matteo.caccin@mail.polimi.it (M. Caccin), massimo.giorgi@mail.polimi.it (M. Giorgi), francesca.giacobbo@polimi.it (F. Giacobbo), mirko.daros@polimi.it (M. Da Ros), mario.mariani@polimi.it (M. Mariani)*

[b] *Milan, Italy, Tel. +39 335 7017918; email: luigi.besozzi@gmail.com*

ABSTRACT

In the nuclear field, the availability of effective techniques to eliminate lead pollution from wastewater is of interest both for the purposes of radiation protection from the radioactive isotope lead-210 and also for the issues related to the use of lead in the new generation reactors nowadays under study. Evidences exist of lead pollution due to the radioactive isotope lead-210 in the proximities of uranium extraction mines. In this study, two commercial granular activated carbons obtained by physical activation of coconut shell, specifically developed and selected to purify potable water from dissolved organics (GCN 1240) and for use in gold recovery systems (GCN 816 G), were studied in batch systems to evaluate their effectiveness for separation of lead (II) from aqueous solutions. A characterization of the two carbons, different in particle size, is provided through determination of their pH_{PZC} and scanning electron microscope analysis. Adsorption of lead (II) was observed as a func-tion of contact time, and its kinetics were fitted. Adsorption data at equilibrium were fitted by isotherm models and the maximum adsorption capacity of the carbons resulted to be 92.39 mg/g (GCN1240) and 32.08 mg/g (GCN 816 G). Experiments were carried out to investigate effects of pH on lead adsorption, evidencing that best removal performances of lead occur near pH 5.0. The present study shows that the considered commercial granular activated carbons can be successfully adopted for removal of lead (II) by adsorption from aqueous solutions.

Keywords: Adsorption; Lead; Granular activated carbon; Batch experiments

1. Introduction

Heavy metal pollution represents a relevant threat for living organisms. Unlike organic pollutants subject to biological degradation, heavy metal ions tend to accumulate in living organisms, potentially leading to diseases [1–4]. Heavy metals mostly considered as potentially toxic for living beings are zinc, cadmium, chromium, copper, mercury, nickel, and lead [5]. Lead poisoning, in particular, may be cause of troubles to kidneys, liver, reproductive system, brain, and central nervous system for human beings [6]; it can likewise become source of diseases such as anemia,

encephalopathy, hepatitis, and nephritic syndrome [7]; behavioral disorders have been also observed in children subject to lead poisoning [8].

Lead poisoning can occur basically through inhalation and swallowing. Inhalation mainly involves workers of industries characterized by long exposures to steams, smokes, and dusts such as metallurgic processes, welding, production of batteries, munitions, pigments, plastic manufactures, and antiradiation screens [9]. Swallowing is mainly connected to the presence of the pollutant in waters, nowadays considered as the main vector of intoxication for human beings [10,11], but it may result dangerous even to aquatic flora and fauna. Lead contamination in waters and wastewaters derives from many types of industry such as electroplating, metal plating, batteries, mining, and tanneries [12]. Other anthropogenic sources of lead pollution include processing and manufacturing of lead products and coal combustion [13].

The problem of lead polluted wastewaters is of interest also in the nuclear field, both for radioprotection concerning the radioactive isotope lead-210 and for toxicity aspects related to the use of lead in the nuclear industry. Significant evidences exist of lead pollution due to the radioactive isotope lead-210 (mostly β^- emitter, $T_{1/2}$ = 22.2 years) in waters in the proximities of uranium extraction mines; lead-210 is among the most radiotoxic elements emitted by coal combustion; further, lead-210 can be found in those materials known as normally occurring radioactive materials (NORM), such as wastes of phosphoric acid production plants, phosphate fertilizers, and zircon sands, used in the production of refractory materials and as well as in ceramic industry. In the nuclear industry, the need for effective lead removal from wastewaters arises from operational activities and/or accidental events involving the heat exchangers of Generation IV lead-cooled fast reactors, currently under study.

Lead can be found in water as Pb^{2+} ions and in mineral or organic–mineral complexes. Diseases have been demonstrated to arise at lead concentrations between 0.01 and 5.0 mg/L [14].

Due to its toxicity, stringent constraints are imposed on lead concentration in industrial wastewaters, in waters for agricultural and recreational employments as well as in drinking water.

At present, the maximum allowable concentration of lead in drinking water has been set by United States Environmental Protection Agency (USEPA) to 0.015 mg/L [15]; concerning industrial wastewaters, the limit established by USEPA is less strict and equal to 0.05 mg/L [16].

To respect limits of lead concentrations, effective techniques for lead removal from waters must be studied and implemented; this need has encouraged a large interest in developing treatment processes such as chemical precipitation, electrochemical reduction, ion exchange, reverse osmosis, membrane separation, biosorption, and adsorption [17–22].

Adsorption is among the most promising processes to purify waters containing heavy metals in traces (ppm or ppb) and in case of limited flow rates [23–28]: in these conditions adsorption is the best choice for lead removal because of its chemical stability, high efficiency, high selectivity, facility of employment, wide range of available adsorbents, and economic fea-sibility. Many studies demonstrate that efficient removal of lead traces can be achieved, making use of activated carbons prepared from a wide range of raw materials. Activated carbon is also particularly suitable for radioactive isotopes removal thanks to its radiation and thermal stability.

Agricultural byproducts of lignocelluloses materials constitute the main sources in the production of commercial activated carbons: many literature studies exist that investigate the adsorption performances of carbons prepared from raw material such as coconut shells [12,29–33], peanut shells [34,35], hazelnut shells [3], nutshells [36], palm shells [37], rice straw [38], and bagasse [39].

Moreover, several studies have been carried out on activated carbons prepared from exotic plants such as *Enteromorpha prolifera* [22], *Polygonum orientale* [17], *Tamarind* wood [13], *Ceiba pentandra* hulls [40], *Firminana simplex* [41], and *Eichhornia* [42]; these sources, although representing important case studies in the field of carbons activation methods, may encounter some difficulties in giving stable and reproducible adsorption results for a commercial utilization.

Lastly, few literature studies about adsorption performances of activated carbons obtained from raw materials of mineral origin also exist: Indonesian peat [43], peat [44], black carbon [45], and brown coal [46]. Some of the literature studies above cited compared adsorption performances of activated carbon "as it is" and activated carbon with improved surface chemical functionality: surface treatments with oxidizing agents (namely H_2O_2 and HNO_3) were found to give a more hydrophilic carbon surface, resulting in a greater chemical affinity toward adsorbate particles [12]; for instance, some positive effects on lead adsorption have been shown when treating carbons surface with Na_2S, because of a good chemical affinity between heavy metals and sulfides [24].

The influence of carbon mass and shaking time on lead adsorption was also studied [42]: removal increases with the mass of activated carbon up to a saturation plateau; lead removal in laboratory batch

mode experiments increases with shaking time up to a limit value. Temperature effects on adsorption of lead were also investigated [22]: adsorption capacity increases with temperature, thanks to a higher diffusion rate of lead ions toward the limit stratum of the adsorbent.

In the present study, adsorption of lead onto two commercially available granular activated carbons, prepared by physical activation of coconut shells, was investigated in batch experiments as a function of contact time and solution pH; kinetics and equilib-rium adsorption isotherms were analyzed to obtain Langmuir and Freundlich constants; adsorption as a function of initial lead concentration and of the dispersed mass of activated carbon was then studied. Activated carbons obtained from coconut shell repre-sent an interesting field of study thanks to their high density, high purity, and low ash content [47]. In particular, the two carbons here studied have been developed and selected to purify potable water from dissolved organics (GCN1240) and for use in gold recovery systems (GCN 816 G), but their adsorption properties for lead were not been investigated so far.

In Section 2, the following points are treated: characteristics of the adsorbents, specification of reagents, and description of the experimental procedure with formulas used for calculations. In subsequent Section 3, experimental characterizations of the activated car-bons, namely pH_{PZC} measurement and scanning elec-tron microscope (SEM) observations of the porous surface, are reported. Results of adsorption experi-ments are then showed and discussed. The main results are then summarized in Section 4.

2. Experimental

2.1. Activated carbons

Two microporous granular activated carbons prepared by physical activation of milled coconut shells were considered, namely GCN1240 and GCN816 G, both supplied by Norit Nederland BV. Some relevant characteristics of the two carbons are reported in Table 1 (GCN1240) and Table 2 (GCN816 G); they are identical for raw material, activation method, and surface functional groups, but different in particle size: GCN1240 has been sieved to particle size ranging between 0.425 and 1.7 mm (equivalent to mesh size range 12–40), while GCN816 G particles range from 1.18 to 2.36 mm (equivalent to mesh size range 8–16).

The adsorption capacity of an activated carbon is mainly determined by its porous structure and surface area, but it is also strongly influenced by the nature of functional groups at the carbon surface. Functional groups can promote bindings by attracting positive charge particles such as metal ions [48].

Table 1
Characteristics of granular activated carbon GCN1240

pH	Alkaline
Apparent density (g/cm^3)	0.51
Density backwashed and drained (g/cm^3)	0.45
Total surface area (B.E.T.) (m^2/g)	1,150
Iodine number	1,050
Ash content (mass-%)	3
Particle size > 1.70 mm (mass-%)	Max. 5
Particle size < 0.425 mm (mass-%)	Max. 5

Table 2
Characteristics of granular activated carbon GCN816 G

pH	Alkaline
Apparent density (g/cm^3)	0.50
Density backwashed and drained (g/cm^3)	N/A
Total surface area (B.E.T.) (m^2/g)	N/A
Iodine number	N/A
Ash content (mass-%)	2
Particle size > 2.36 mm (mass-%)	Max. 1.5
Particle size < 1.18 mm (mass-%)	Max. 1

Measurements of the pH_{PZC} of the two carbons were performed, in order to prove the alkaline nature of their surface. The morphologic characteristics of the surface and the porous structure of the adsorbents were then observed making use of a SEM.

2.2. Reagents

As the adsorption behavior doesn't change with the type of lead isotope considered, stock solutions with stable isotopes of lead were prepared to investigate the removal of lead from aqueous solutions. Stock solutions of lead (II) were prepared by dissolving analytical grade lead nitrate $Pb(NO_3)_2$ in ultrapure water (Millipore MilliQ water) at the desired initial concentrations. Two reasons justify why lead (II) nitrate was chosen as lead-containing solution: (a) nitrate salt is a very water-soluble lead compound, so it guarantees great availability of dissociated lead (II) ions in solution; (b) NO_3^- nitrate ion is the conjugate base of the HNO_3 strong acid: it is a very weak base and do not produce hydrolysis, this means it cannot affect pH, or lead adsorption during experiments.

2.3. Batch adsorption experiments

Adsorption experiments were carried out by batch techniques. Activated carbon was kept in contact with

the solution containing metal ions in 30 mL Erlenmeyer flasks; pH was adjusted by adding HNO_3 or NaOH to the optimal value; the content was mixed with a constant stirring rate of 120 rpm. After shaking, the activated carbon was separated from the supernatant at preset times, aqueous samples were taken and the residual metal concentrations were analyzed using a Thermo Fisher X Series II model ICP mass spectrometer (each sample was read five times to get the average value). The amount of adsorbed pollutant was determined by the difference between the initial and the residual metal concentrations in aqueous solution.

The amount of metal ion adsorbed at time t, here called q_t [mg/g], was calculated from the mass balance equation

$$q_t = \frac{(c_0 - c_t) \cdot V}{W} \quad (1)$$

where c_0 and c_t are the initial metal concentration and the residual metal concentration in the solution [mg/L], respectively, V is the volume of solution [L], and W is the mass of activated carbon [g]. If t is equal to the equilibrium contact time, then $c_t = c_e$, $q_t = q_e$, and the amount of metal ion adsorbed at equilibrium, q_e, is calculated using Eq. (1). The removal efficiency R [%] was calculated from the equation

$$R = 100 \times \frac{(c_0 - c_t)}{c_0} \quad (2)$$

3. Results and discussion

3.1. Speciation of lead in aqueous solution

Lead nitrate in aqueous solution dissociates into Pb^{2+} and NO_3^- ions. Pb^{2+} ions constitute a Lewis acid forming coordinate covalent bonds with the surrounding water molecules i.e. acid hydrolysis takes place; for metals with multiple charge, such as lead, consecutive hydrolysis reactions easily occur, leading to new complex species coordinated by one or more Pb^{2+} cations.

In particular, literature studies report formation and stability constants of seven different species of lead in water solution depending on pH and lead (II) concentration: in correspondence of low concentrations of lead, mononuclear complexes such as $PbOH^+$, $Pb(OH)_2$, and $Pb(OH)_3^-$ tend to form by hydrolysis; whereas, at high lead concentrations, a relevant formation of polinuclear species containing more than one lead ion may be observed, such as Pb_2OH^{3+}, $Pb_3(OH)_4^{2+}$, $Pb_4(OH)_4^{4+}$ and $Pb_6(OH)_8^{4+}$ [39,49].

A lead speciation profile, for lead concentrations of interest for the purpose of this study (100 mg/L at a temperature of 23 ℃) was drawn making use of MINTEQA2 simulation software distributed by USEPA, a speciation model for diluted aqueous systems at equilibrium based on a thermodynamic database. The speciation profiles calculated by the software are reported in Figs. 1 and 2. Fig. 1 shows the presence of lead in aqueous phase up to pH near to 6; then, formation of solid $Pb(OH)_2$ occurs due to precipitation of lead as hydroxide, causing the aqueous phase to reduce to extremely low molar concentrations (about 10^6 times lower than the solid phase concentration). Fig. 2 shows the speciation profile of lead only inherent to the aqueous phase which is 10^6 times lower than the solid phase when pH > 7. It can be seen that the presence of polinuclear complex species is here absolutely negligible, proving that we are in the case of low lead concentrations; what is worthy of note is the presence of some mononuclear species, although low in terms

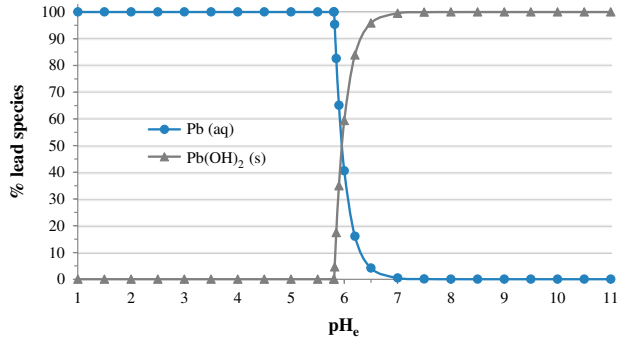

Fig. 1. MINTEQA2 speciation profile of lead at varying equilibrium pH values.

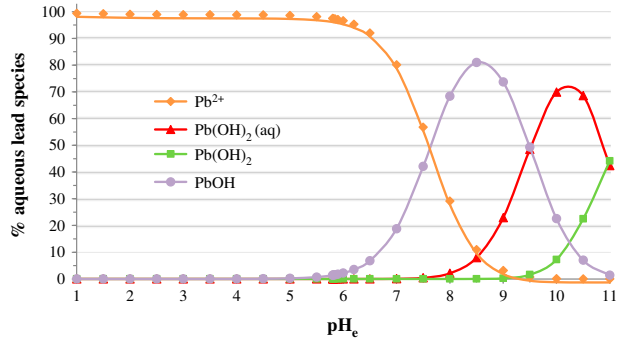

Fig. 2. MINTEQA2 speciation profile of lead in the aqueous phase at varying equilibrium pH values.

of molar concentrations: while at pH values between 1 and 6, the dominant form is the dissolved cation Pb^{2+}, at higher pH values, it can be observed a formation of $PbOH^{+}$, $Pb(OH)_2$, and $Pb(OH)_3^{-}$.

In conclusion, the relevant information to the purpose of interest are: (a) aqueous lead as Pb^{2+} ions exists at pH values lower than the value at which precipitation of lead hydroxide occurs; (b) solid lead tends to form at higher pH values.

3.2. GCN1240 adsorbent analysis

3.2.1. pH_{PZC} measurement

The pH_{PZC} (point of zero charge) of the GCN1240 activated carbon surface was measured with the pH drift method [50,51]. Known amounts of activated car-bon were sequentially added to a given volume (40 mL) of NaCl solution 0.1 M; after each addition, the dispersion was agitated for 15 min on a magnetic stirrer and its pH value was measured by using a dig-ital pH-meter. In correspondence with the increasing mass of activated carbon, a progressive increase in the pH values of the solution was observed, up to the achievement of a plateau, defining the pH_{PZC}. A pH_{PZC} = 10.22 was found, confirming the alkaline nat-ure of the surface of GCN1240.

The point of zero charge corresponds to the pH of the solution at which the carbon presents zero net charge on its surface [12]. If the solution pH is under the pH_{PZC} value, an excess of dissolved H^{+} ions will tend to diffuse to the boundary layer of the surface, which will tend to positively charge; whereas, above the value of pH_{PZC}, an increase of negative charge on the surface will take place. Hence, it is possible to affirm that pH_{PZC} influences the carbon selectivity toward specific species: for this reason, the pH_{PZC} should be taken into account when considering effects of pH on adsorption.

3.2.2. SEM observations

SEM observation reported in Fig. 3 clearly shows the porous structure of the carbon GCN1240 (10,000× enlargement). It is possible to notice the pres-ence of macropores having size greater than 50 nm; whereas it is not possible to see meso and micropores because they belong to the internal structure of the adsorbent. Fig. 4 (30,000× enlargement) and Fig. 5 (100,000× enlargement) show the carbon surface with higher magnification; to be noticed the presence of carbon powder which appears white-colored because electrostatically charged.

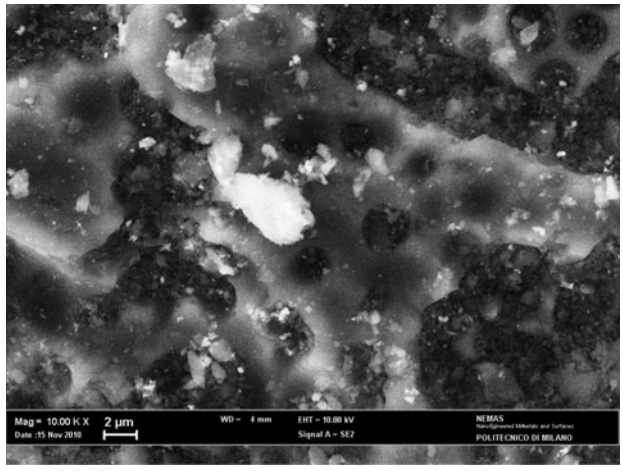

Fig. 3. SEM photograph of granular activated carbon GCN1240 (10,000×) [53].

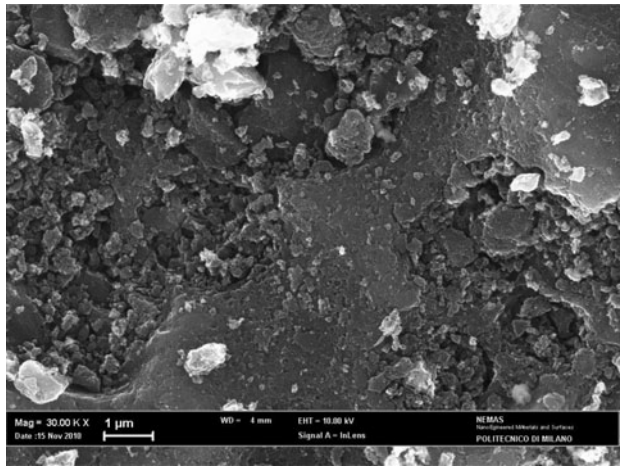

Fig. 4. SEM photograph of granular activated carbon GCN1240 (30,000×) [53].

It is appropriate to mention a particularly relevant property of the GCN1240 taken from the datasheet of the carbon: its total specific surface area measures 1,150 m^2/g (Table 1), which is quite a high value; the total specific surface area is normally determined by fit-ting experimental data obtained from adsorption of N_2 (at a temperature of 77 K) with the BET equation [52].

3.3. Lead adsorption on GCN1240

3.3.1. Effect of pH on adsorption of lead

The removal efficiency of Pb^{2+} ions is strongly influenced by the pH of the solution. In order to study this influence, adsorption experiments (initial lead

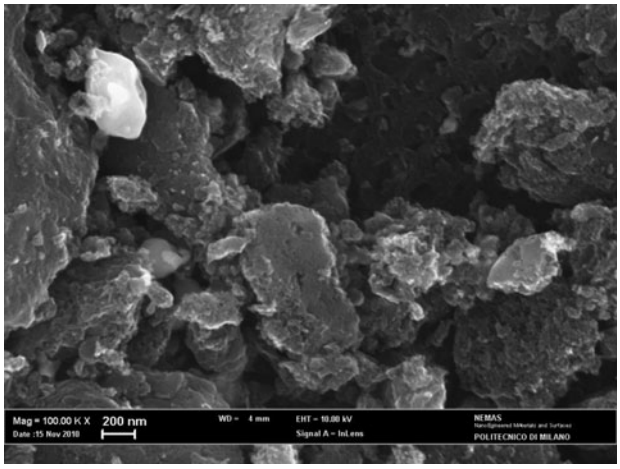

Fig. 5. SEM photograph of granular activated carbon GCN1240 (100,000×) [53].

concentration of 30 mg/L; carbon mass of 20 mg; contact time of 24 h) were conducted at different pH val-ues, by adding an appropriate quantity of HNO_3 or NaOH to the samples. Results are shown in Fig. 6, representing removal efficiency of Pb^{2+} vs. pH of solu-tion: lead removal resulted strongly affected by pH.

At very acid pH values (minor than 4), no removal of lead occurs: this behavior can be explained by a competition between Pb^{2+} ions and H^+ ions in the occupation of the microporous sites on the carbon. At increasing pH values (about 5), hydrogen ions disappear from the solution and from the carbon surface too, leaving sites free and therefore available for lead ions. This experimental evidence suggests that a mechanism of ion exchange H(I)/Pb(II) could take place in the lead adsorption process. In addition, at these pH values, the negative charge on the surface of the carbon tends to increase, because its functional groups become subject to deprotonation subsequent to a poor concentration of H^+ ions in the bulk respect to the one

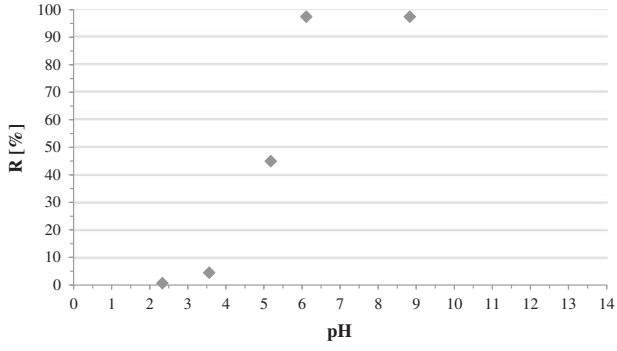

Fig. 6. Effect of pH on lead adsorption on GCN1240 (c_0 = 30 mg/L; W = 20 mg).

existing at very acid pH values: hence, while surface negative charge increases, lead (II) ions become subject to a greater electrostatic attraction, favoring the adsorption process [17].

At basic pH values, a removal efficiency near to 100% occurs due to precipitation of lead (II) hydroxide $Pb(OH)_2$. Now, although hydroxide precipitation permits to obtain an effective lead removal from the solution—to the extent that solubility equilibria are nowadays the core of separation techniques of huge employment—it appears as an undesired effect when the purpose is to evaluate what fraction of pollutant is actually removed by adsorption.

Moreover, when operating in dynamic conditions via column adsorption procedures, the precipitation may cause the clogging of the carbon matrix with a consequent decrease of the removal efficiency of the apparatus. Considering what above said, the optimal pH value is the higher possible value below the pH of lead (II) hydroxide precipitation (the theoretical pH of precipitation for a starting lead (II) concentration of 30 mg/L is 6.0).

Therefore, for this work, it was chosen to perform adsorption experiments keeping the natural pH of the lead-containing solution, which is above 5.0, and remaining below the precipitation pH value.

3.3.2. SEM images and elemental analysis of precipitate on GCN1240

To produce evidence of the occurring formation of $Pb(OH)_2$ precipitate on the carbon, SEM images were taken after an adsorption experiment with initial lead concentration of 80 mg/L. The theoretical precipitation pH value of lead hydroxide for a lead concentration of 80 mg/L is 5.78. After an experiment conducted under conditions of pH not controlled (24 h of contact time), it was measured a pH 5.92 with a digital pH-meter, which is over the precipitation value: so, a formation of solid lead is expected to occur on the carbon sur-face. SEM images reported in Fig. 7 (1,000× enlarge-ment), Fig. 8 (5,000× enlargement), Fig. 9 (10,000× enlargement) clearly show the presence of solid Pb $(OH)_2$ hexagonal crystals having dimensions in the order of some μm.

To confirm that those crystals are made of lead, an elemental analysis was performed. The elemental analysis, performed on a portion of carbon covered by hexagonal crystals, evidenced three peaks corresponding to carbon, oxygen, and lead elements, while on a portion of carbon surface not covered by hexagonal crystals, only the peak corresponding to the carbon element appeared.

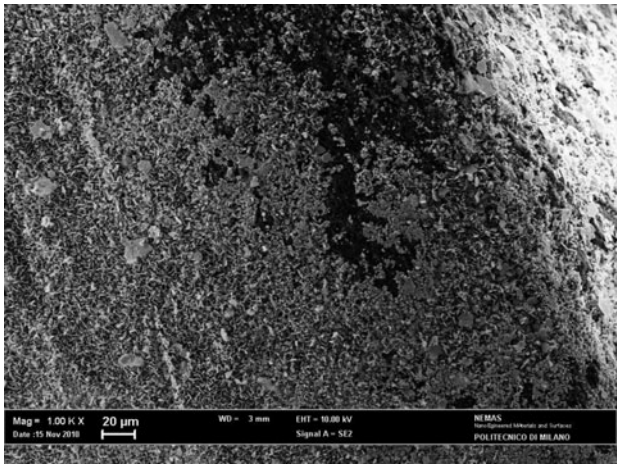

Fig. 7. $Pb(OH)_2$ precipitate on GCN1240 (1,000×).

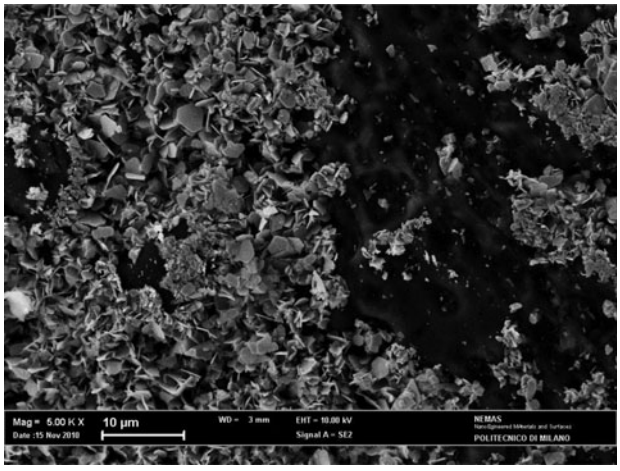

Fig. 8. $Pb(OH)_2$ precipitate on GCN1240 (5,000×).

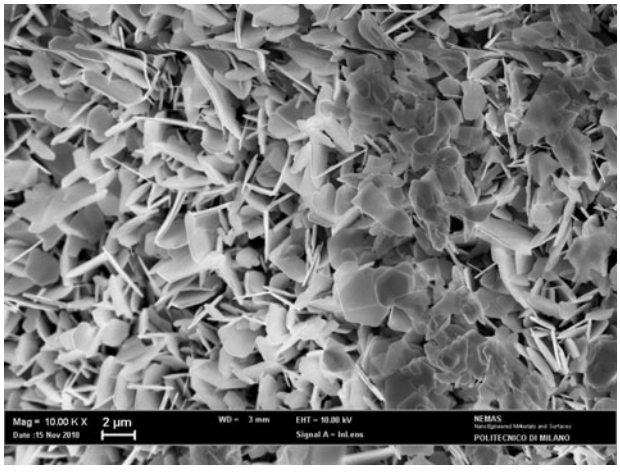

Fig. 9. $Pb(OH)_2$ precipitate on GCN1240 (10,000×).

3.3.3. *Effect of contact time on adsorption of lead*

Adsorption experiments were carried out for con-tact times ranging from 8 to 96 h with fixed mass of adsorbent (30 mg) and initial lead (II) concentration (100 mg/L), at T = 296.15 K. As shown in Fig. 10, the adsorption equilibrium was reached after 40 h: this value has been taken as the equilibrium time.

3.3.4. *Adsorption kinetics of lead*

Kinetic models are used to fit experimental data, in order to examine the controlling mechanism of the adsorption process. To this purpose, experimental data were fitted with the following pseudo-first-order model

$$\frac{dq_t}{dt} = K_1 \cdot (q_e - q_t) \tag{3}$$

where K_1 is the Lagergren rate constant [h^{-1}]; q_t and q_e are the adsorption capacities at time t and at equilibrium [mg/g], respectively. Integrating and applying the initial condition $q_t(0) = 0$, Eq. (3) becomes

$$\log_{10}(q_e - q_t) = \log_{10} q_e - \frac{K_1}{2.303} \cdot t \tag{4}$$

Experimental data were also fitted with a pseudo-second-order model, following the equation

$$\frac{dq_t}{dt} = K_2 \cdot (q_e - q_t)^2 \tag{5}$$

where K_2 [g/(mg h)] is the rate constant of pseudo-second-order; by integrating Eq. (5) with the initial condition $q_t(0) = 0$, we obtain

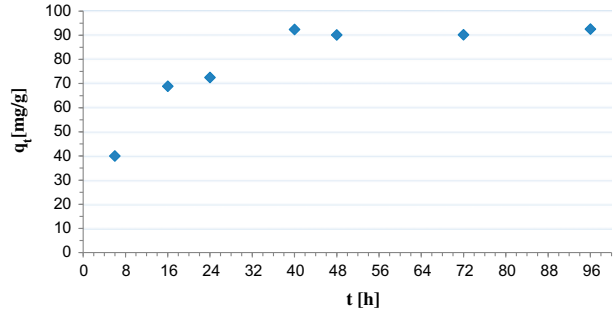

Fig. 10. Effect of contact time on lead adsorption on GCN1240 (c_0 = 100 mg/L; W = 30 mg).

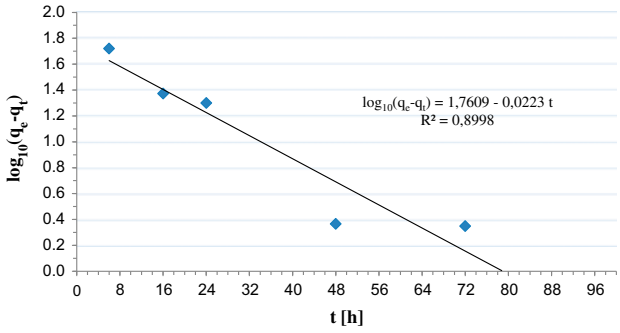

Fig. 11. Pseudo-first-order model for lead adsorption on GCN1240.

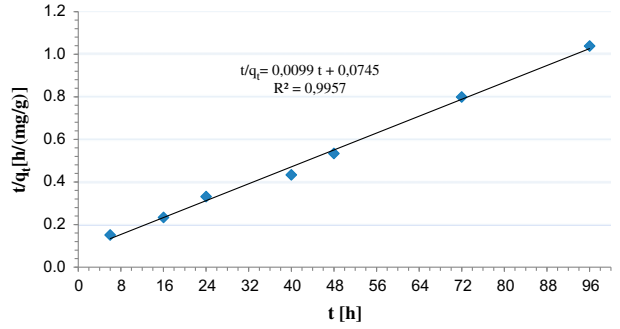

Fig. 12. Pseudo-second-order model for lead adsorption on GCN1240.

$$\frac{t}{q_t} = \frac{t}{q_e} + \frac{1}{K_2 \cdot q_e^2} \tag{6}$$

Fits of experimental data with the pseudo-first-order and pseudo-second-order models are reported in Figs. 11 and 12, respectively. The values of K_1, K_2, and q_e were calculated from the slopes and the intercepts of the straight lines resulting from the fits: these val-ues are listed in Table 3 for both the models, in addi-tion to the R^2 values. Lead adsorption onto the activated carbon seems to better follow a pseudo-second-order kinetic: in fact, the experimental value of q_e is very near to the calculated one for this model and the corresponding R^2 value results to be higher.

3.3.5. *Adsorption isotherms of lead*

The experimental results concerning the adsorption of lead at equilibrium time (40 h at 293.15 K, Fig. 10) have been interpreted according to Langmuir and Freundlich adsorption isotherms.

According to the Langmuir model, adsorption occurs uniformly on the active sites of the adsorbent; once an adsorbate particle occupies a site, no further adsorption can take place at that site. The Langmuir model is represented by the following equation:

$$\frac{c_e}{q_e} = \frac{c_e}{q_{\max}} + \frac{1}{q_{\max} \cdot K_L} \tag{7}$$

where $q_{\max}$ is the maximum monolayer adsorption capacity of the adsorbent and K_L is the Langmuir constant related to the free energy of adsorption.

A plot of c_e/q_e vs. c_e results in a straight line with a slope of $1/q_{\max}$ and intercept of $1/(q_{\max} \cdot K_L)$, as shown in Fig. 13.

The equation representing the Freundlich model, which is suitable for adsorbents with a highly heterogeneous surface, can be written in the linearized form

$$\log_{10} q_e = \log_{10} K_F + \frac{1}{n} \cdot \log_{10} c_e \tag{8}$$

where K_F [mg/(g·(mg/L)$^{1/n}$)] and $1/n$ are Freundlich constants related to the adsorption capacity and the adsorption intensity, respectively.

A plot of $\log_{10}(q_e)$ vs. $\log_{10}(c_e)$ is shown in Fig. 14: it results in a straight line with a slope of $1/n$ and intercept of $\log_{10}(K_F)$.

Fig. 15 reports a comparison between the adsorption isotherm models and the experimental data. Values of Langmuir and Freundlich constants are

Table 3
Pseudo-first-order and pseudo-second-order constants, and R^2 value for lead (II) adsorption on GAC GCN1240

Pseudo-first-order	q_e exp (mg/g)	q_e calculated (mg/g)	K_1 (h^{-1})	R^2
	92.39	57.66	0.05	0.90
Pseudo-second-order	q_e exp (mg/g)	q_e calculated (mg/g)	K_2 [g/(mg h)]	R^2
	92.39	101.01	1.31×10^{-3}	0.996

Note: A comparison between the values of q_e calculated from the models and the experimental values of q_e is also given.

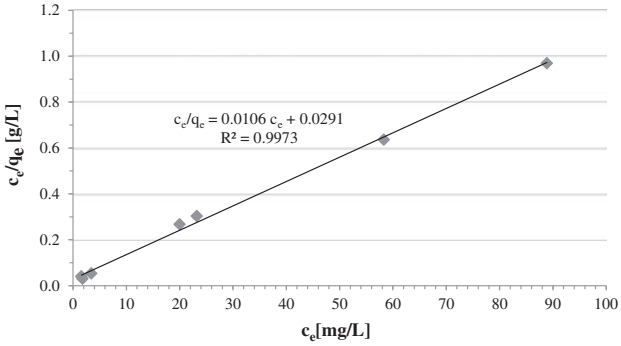

Fig. 13. Langmuir adsorption isotherm of lead on GCN1240.

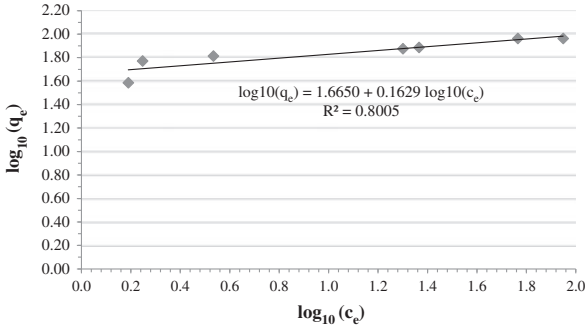

Fig. 14. Freundlich adsorption isotherm of lead on GCN1240.

reported in Table 4. Maximum experimental adsorp-tion capacity was 92.39 mg/g, confirming that the granular activated carbon GCN1240 can be effectively used for lead removal from aqueous solutions; in fact, it presents very good lead adsorption performances in comparison with other adsorbents reported in litera-ture and listed in Table 5.

3.3.6. Effect of initial lead concentration on adsorption

The effect of lead concentration was studied using three different lead-containing solutions with concentrations between 40 and 150 mg/L, at a fixed mass of activated carbon (30 mg). Fig. 16 shows that adsorption capacity at equilibrium increases as initial lead concentration increases. High lead concentra-tions tend to increase the concentration gradient of Pb^{2+} ions toward the boundary layer of the adsorbent surface, increasing the diffusive flow and giving the carbon a greater adsorption capacity at equilibrium [40].

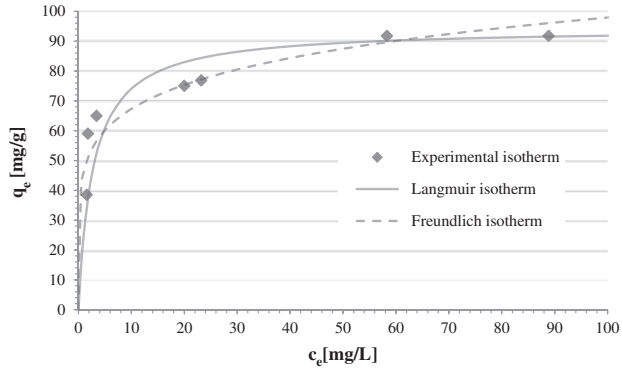

Fig. 15. Lead adsorption isotherms on GCN1240.

Table 4
Langmuir and Freundlich constants calculated from lead adsorption data on GCN1240

Langmuir	q_{max} (mg/g)	K_L (L/mg)	R^2
	94.34	0.36	0.998
Freundlich	$1/n$	K_F [mg/(g (mg/L)$^{1/n}$)]	R^2
	0.16	46.24	0.805

3.3.7. Effect of carbon mass on adsorption of lead

Effect of the concentration of activated carbon on lead removal efficiency was observed by executing batch adsorption experiments at fixed initial lead concentration (100 mg/L) and varying the mass of carbon in the dispersion. Removal efficiencies found at equilibrium are plotted in Fig. 17. The results show that the removal efficiency increases with the concentration of activated carbon due to more total surface area available (i.e. a greater number of surface functional groups) and to a larger available microporous volume (i.e. a greater number of active adsorption sites) [22].

3.4. GCN816 G adsorbent analysis

3.4.1. pH_{PZC} measurement

The GCN816 G carbon is similar to the GCN1240 in raw material (coconut shell), and activation method (physical), but is characterized by a bigger particle size.

A characterization of GCN816 G was carried out by measuring the pH value corresponding to the point of zero charge, using the same method used for GCN1240. The GCN816 G activated carbon shows a pH_{PZC} equal to 9.43, confirming an alkaline surface.

This result allows to affirm that, working in a lead-containing solution with a pH value lower than 9.43,

Table 5
Lead adsorption results in some literature studies

Adsorbent	Particle size (mm)	Max adsorption capacity (mg/g)	Equilibrium time	pH	Refs.
Coconut shell (commercial)	0.25/0.30	17.19	48 h	4	Song et al. [12]
Coconut shell (commercial) treated with HNO_3	0.25/0.30	40.12	48 h	4	Song et al. [12]
Palm shell (commercial)	0.8/1	95.20	–	5	Issabayeva et al. [37]
Coconut shell (commercial)	0.85/2.36	21.88	–	5	Goel et al. [29]
Coconut shell (commercial) treated with Na_2S	0.85/2.36	29.44	–	5	Goel et al. [29]
Coconut shell	0.053/0.85	26.50	2 h	4.5	Sekar et al. [30]
Hazelnut shell	0.5/2	13.05	1 h	5.7	Imamoglu and Tekir [3]
Almond shell	0.49/1	22.7	50 h	–	Ferro-Garcia et al. [55]
Olive stones	0.49/1	18.3	50 h	–	Ferro-Garcia et al. [55]
Peach pit	0.49/1	17.5	50 h	–	Ferro-Garcia et al. [55]
Indonesian peat	0.15	79.68	3.5 h	6	Balasubramanian et al. [43]
Peat	0.5/0.71	122	4 h	–	Ho and McKay [44]
Sea-buckthorn activated with phosphoric acid	0.25/0.42	51.81	10 min	5–7	Mohammadi et al. [56]
Sea-buckthorn activated with zinc chloride	0.25/0.42	25.91	15 min	6–7	Mohammadi et al. [56]
Enteromorpha prolifera	0.125	146.85	40 min	5	Li et al. [22] Wang
Polygonum orientale	0.09	98.39	15 min	5	et al. [17] Acharya
Tamarind wood	50.8/76.2	43.85	1 h	6.5	et al. [13] Rao et al.
Ceiba pentandra hulls	0.15	25.5	50 min	6	[40] Shekinah et al.
Eichhornia	0.125/0.18	16.61	125 min	3	[42] Patnukao et al.
Eucalyptus Camaldulensis Dehn.	0.045/0.15	113.96	45 min	5	[54] Qiu et al. [45]
Black carbon (commercial)	–	112.92	48 h	4.8	
Brown coal	0.5/1	53.87	1 h	–	Simonova et al. [46]
Fly ash	–	10	3 h	4.5	Cho et al. [57]
Sawdust	0.25/0.59	3.19	–	–	Yu et al. [58]
Coconut shell (commercial, Norit GCN816 G)	1.18/2.36	32.08	96 h	5	This study
Coconut shell (commercial, Norit GCN1240)	0.425/1.7	92.39	40 h	5	This study

the surface shows a tendency to positively charge by attracting cations, such as Pb^{2+}.

3.4.2. SEM observations

SEM observations of the GCN816 G surface were performed. In Fig. 18 (1,000× enlargement), the analyzed carbon particle shows the presence of two different areas: one in which surface appears very rough, and the other one characterized by a smooth surface on which macropores conducting toward the internal structure of the carbon are well visible. This different morphology visible, thanks to the greater particle size of this carbon, can be linked to the peculiar "tile" shape of carbon granules obtained from coconut shells.

Fig. 19 (2,000× enlargement) better shows the area having smooth surface, when irregular pores are well visible; a further enlargement (10,000× enlargement) showed in Fig. 20 allows to distinguish the internal porous structure, with diameter at the entrance of about 2 μm.

Fig. 21 eventually shows an enlargement (5,000×) of the mentioned area with rough surface.

3.5. Lead adsorption on GCN816 G

3.5.1. Effect of contact time on adsorption of lead

In order to evaluate the time required for the adsorbent–adsorbate system to reach equilibrium, adsorption experiments were carried out for contact

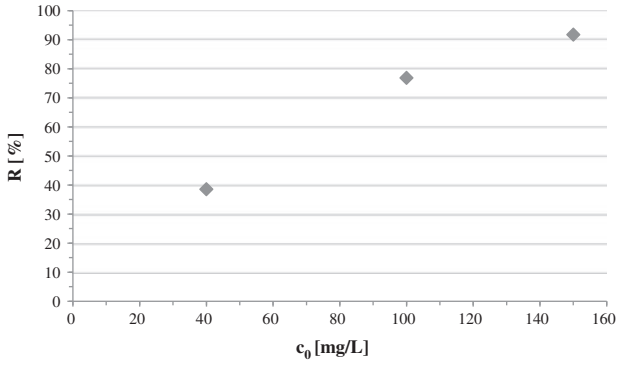

Fig. 16. Effect of initial lead concentration on adsorption on GCN1240 (W = 30 mg).

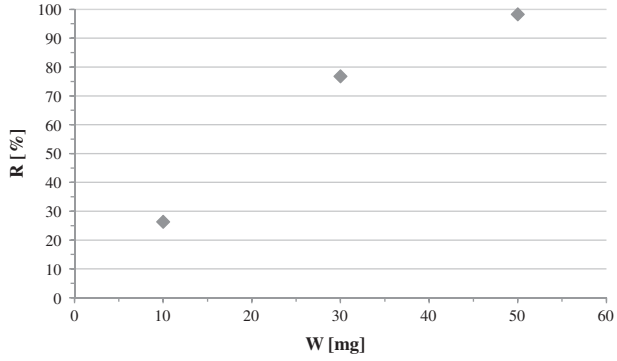

Fig. 17. Effect of carbon mass on lead removal efficiency on GCN1240 (c_0 = 100 mg/L).

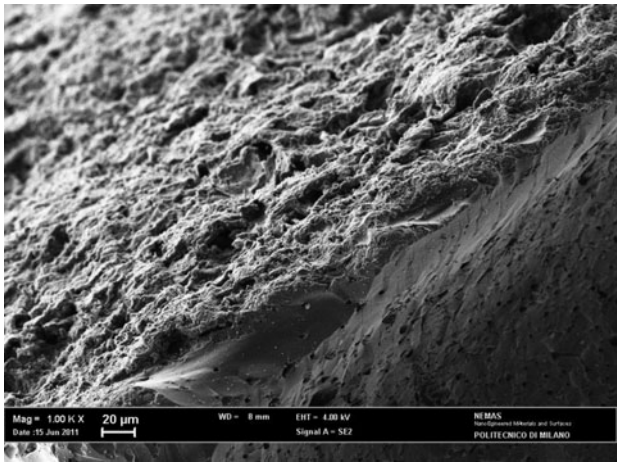

Fig. 18. SEM photograph of granular activated carbon GCN816 G (1,000×).

times ranging from 4 to 144 h, maintaining constant the mass of adsorbent and initial lead (II) concentration at T = 296.15 K. To better study the kinetics of the adsorption process on this carbon, two couples of c_0-W associations were adopted to observe lead adsorption as a function of time: in the first series of samples, an initial lead concentration c_0 = 40 mg/L and a mass car-bon W = 30 mg were adopted, while the second series of samples was carried out using c_0 = 100 mg/L and W = 50 mg. Results plotted in Fig. 22 show that the adsorption equilibrium was reached after 96 h, suggesting that adsorption of lead on this carbon, with big particles size, is a slow process. In the following, 96 h was taken as the equilibrium time.

Anyway, the adsorption capacity after 48 h was 91% of the adsorption capacity at equilibrium concerning the series c_0 = 40 mg/L and W = 30 mg, and 87%

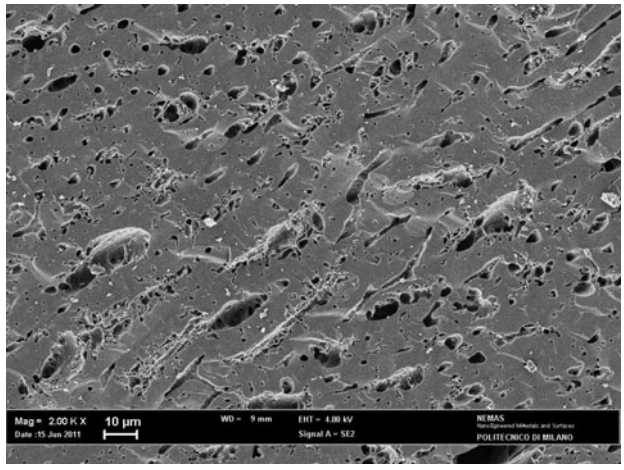

Fig. 19. SEM photograph of granular activated carbon GCN816 G (2,000×).

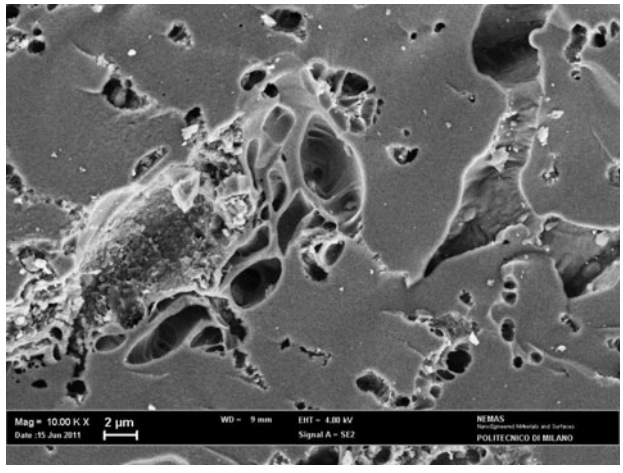

Fig. 20. SEM photograph of granular activated carbon GCN816 G (10,000×).

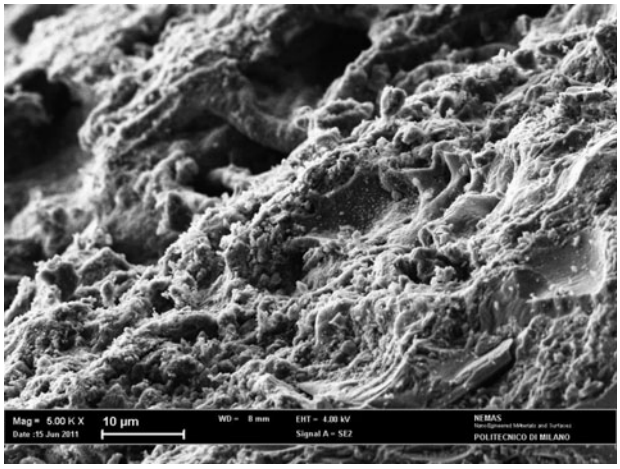

Fig. 21. SEM photograph of granular activated carbon GCN816 G (5,000×).

of the equilibrium adsorption capacity concerning the series c_0 = 100 mg/L and W = 50 mg, with the advantage to cut in half the duration of the adsorption procedure.

Moreover, from Fig. 22, it can be inferred that the initial removal process is fast due to the high concentration gradient existing between the bulk and the boundary layer of the adsorbent surface and to a greater availability of active sites on the carbon surface. For longer times, the removal process velocity becomes slower, because lead ions diffuse more slowly toward the boundary layer and the total available microporous surface area tends to diminish [22].

3.5.2. *Adsorption kinetics of lead*

Kinetic models are used to fit experimental data, in order to examine the controlling mechanism of the adsorption process. To this purpose, experimental data were fitted with a pseudo-first-order model (Eq. (4)) and a pseudo-second-order model (Eq. (6)).

Fits of experimental data with the pseudo-first-order and pseudo-second-order models are reported in Figs. 23 and 24 concerning the sample ser-ies c_0 = 40 mg/L and W = 30 mg, and in Figs. 25 and 26 for the sample series c_0 = 100 mg/L and W = 50 mg, respectively. The values of K_1, K_2, and q_e were calculated from the slopes and the intercepts of the straight lines resulting from the fits: these values are listed in Table 6 for both the models and the series of samples, in addition to the R^2 values. Lead adsorp-tion onto GCN816 G seems to better follow a pseudo-second-order kinetic: this can be said considering that the experimental value of q_e is very near to the calcu-lated one for this model, and the R^2 value results to be higher for both the series of samples.

3.5.3. *An investigation on the adsorption mechanism*

The very slow kinetic of GCN816 G (equilibrium time of about 96 h, Fig. 22) allows to perform an investigation of the adsorption mechanism based on the intraparticle diffusion model. Experimental data obtained for the kinetic study are useful to get some information on the dynamics of the adsorption process. An adsorption reaction can be summarized into the following steps:

(1) the ion leaves the bulk toward the boundary layer of the adsorbent surface;
(2) film diffusion: the ion migrates through the boundary layer toward the external surface of the adsorbent;
(3) particle diffusion: the ion is transferred from the surface to the intraparticle active sites; and
(4) the ion is adsorbed on active sites of the adsorbent.

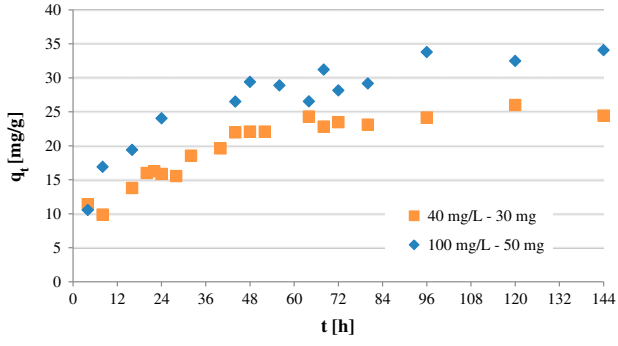

Fig. 22. Effect of contact time on lead adsorption on GCN816 G (square series: c_0 = 40 mg/L, W = 30 mg; diamond series: c_0 = 100 mg/L, W = 50 mg).

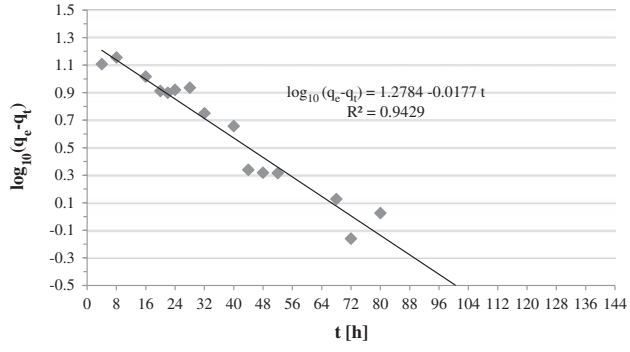

Fig. 23. Pseudo-first-order model for lead adsorption on GCN816 G (c_0 = 40 mg/L; W = 30 mg).

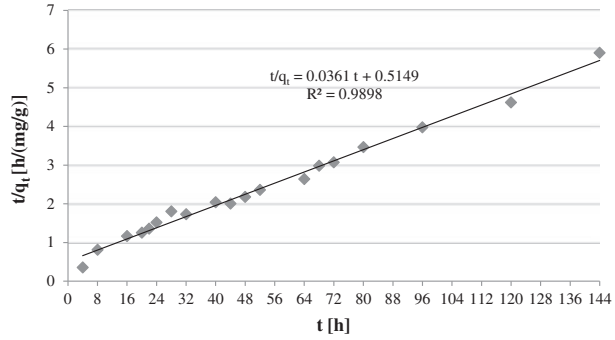

Fig. 24. Pseudo-second-order model for lead adsorption on GCN816 G (c_0 = 40 mg/L; W = 30 mg).

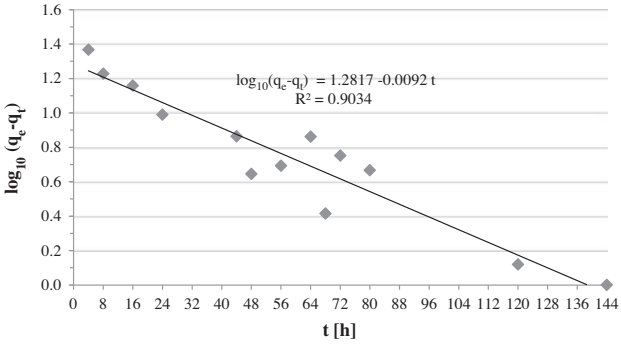

Fig. 25. Pseudo-first-order model for lead adsorption on GCN816 G (c_0 = 100 mg/L; W = 50 mg).

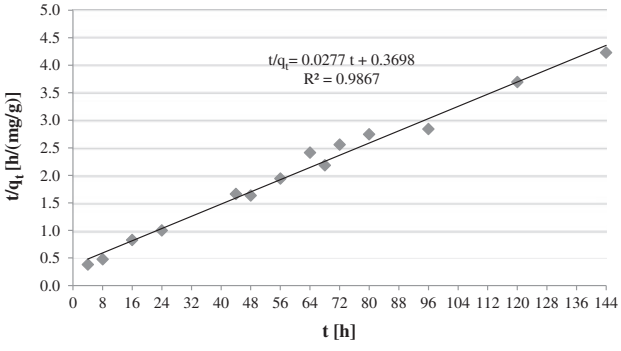

Fig. 26. Pseudo-second-order model for lead adsorption on GCN816 G (c_0 = 100 mg/L; W = 50 mg).

Since the first step does not involve the adsorbent and the fourth step is a very rapid process, it is possible to exclude their relevance on the reaction kinetics. To determine what influence film diffusion and particle diffusion steps have on the kinetics, the following intraparticle diffusion model proposed by Weber and Morris is largely employed [22]:

$$q_t = K_{ID} \cdot t^{1/2} + c_i \quad (9)$$

where K_{ID} is the kinetic constant of intraparticle diffusion relative to the generic step i of the adsorption process [mg/(g $h^{1/2}$)], and c_i is the intercept on the y-axis of such step. Values of c_i contain information about the thickness of the boundary layer because a high value of the intercept may be indicative of an important effect of the boundary layer. On the basis of the intraparticle diffusion model, a plot was drawn reporting experimental values of q_t (both for the series c_0 = 40 mg/L, W = 30 mg and for the series c_0 = 100 mg/L, W = 50 mg) vs. $t^{1/2}$: a linear fit of such plot, shown in Fig. 27, allowed to estimate the model parameters K_{ID} and c_i. The obtained multilinear plot suggests the fact that in the adsorption process both the two above mentioned steps occurred. For both the series of samples, the first portion of the plot repre-sents adsorption occurring during the film diffusion step, i = 1, while the second portion describes the step, more gradual, of intraparticle diffusion, i = 2. Parame-ters of the model were calculated and shown in Table 7. For both the initial lead concentrations, it resulted $K_{ID1} > K_{ID2}$ and $c_1 > c_2$. This gives an analyti-cal piece of information concerning the fact that in the first step (lower times) a faster removal of lead was observed: at first times, there is more surface area available and adsorption reaction is dominated by the speed at which lead ions reach the surface. When the adsorbate accumulating on the surface obstructs the arrival of further ions, the reaction is then domi-nated by the speed at which adsorbed ions diffuse from external sites to the internal ones [17].

3.5.4. Effect of pH on adsorption of lead

Influence of pH on removal efficiency of Pb^{2+} ions was investigated for the activated carbon GCN816 G. Adsorption experiments at equilibrium (96 h) were executed at varying pH values with initial lead concentration of 100 mg/L, carbon mass equal to 50 mg; pH was adjusted by adding an appropriate quantity of HNO_3 or NaOH to the samples. Results are reported in Fig. 28, which shows removal efficiency of Pb^{2+} vs. the pH of solution: it is apparent that removal of lead is affected by the pH of the solutions.

At pH values below 3, no removal of lead occurs, due to competition between H^+ and Pb^{2+} ions. At pH values near to 4–5, lead removal increases thanks to a probable mechanism of ion exchange H(I)/Pb(II). At basic pH values, a removal efficiency near to 100%occurs due to precipitation of lead (II) hydroxide Pb $(OH)_2$ (as already seen for GCN1240), due to the fact

Table 6
Pseudo-first-order and pseudo-second-order constants, and R^2 value for lead (II) adsorption on GAC GCN816 G

Pseudo-first-order	q_e exp (mg/g)	q_e calculated (mg/g)	K_1 (h^{-1})	R^2
40 mg/L–30 mg	24.15	18.98	0.04	0.94
100 mg/L–50 mg	33.79	19.13	0.02	0.90
Pseudo-second-order	q_e exp (mg/g)	q_e calculated (mg/g)	K_2 [g/(mg h)]	R^2
40 mg/L–30 mg	24.15	27.70	2.53×10^{-3}	0.9898
100 mg/L–50 mg	33.79	36.10	2.07×10^{-3}	0.9867

Note: A comparison between the values of q_e calculated from the models and the experimental values of q_e is also given.

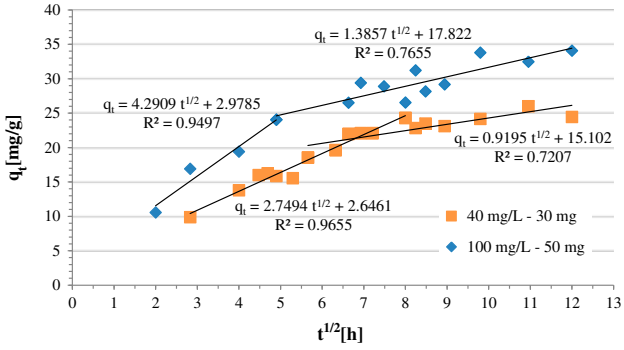

Fig. 27. Intraparticle diffusion model for lead adsorption kinetics on GCN816 G (square series: c_0 = 40 mg/L, W = 30 mg; diamond series: c_0 = 100 mg/L, W = 50 mg).

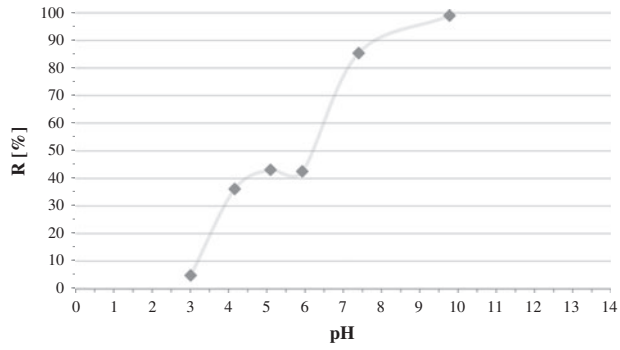

Fig. 28. Effect of pH on lead adsorption on GCN816 G (c_0 = 100 mg/L; W = 50 mg).

that, for a starting lead (II) concentration of 100 mg/L, the theoretical pH of precipitation for lead hydroxide is 5.74.This information enables to distinguish between removal due to adsorption and removal due to precipitation of lead hydroxide, therefore, in this case, the optimal pH to perform adsorption is between 4 and 6.

For this reason, in the following, adsorption experiments with initial and final pH values below the theoretical pH of precipitation of lead hydroxide were considered significant for investigations on the adsorption process. The pH values were measured at the end of each adsorption experiment due to the alkaline nature of the activated carbon that tends to change the pH of the dispersion toward alkaline values.

As a general rule to allow adsorption and to avoid precipitation, the mass of activated carbon used should be carefully evaluated to avoid precipitation.

3.5.5. SEM images and elemental analysis of precipitate on GCN816 G

SEM images were taken of a carbon sample after an equilibrium adsorption experiment (initial concentration of 100 mg/L, carbon mass of 50 mg) in which pH had been adjusted to 7.0 by adding NaOH and the removal observed was of 25 mg/g. Since the experiment was conducted at pH values above the precipitation value of the lead hydroxide, SEM analysis evidenced a carbon surface completely obstructed by lead crystals, as visible in Fig. 29 (1,000× enlargement) and Fig. 30 (5,000× enlargement). Confirming that crystals are $Pb(OH)_2$ precipitate, the elemental superficial analysis showed presence of lead, oxygen, and carbon elements on the activated carbon surface.

For comparison, a carbon particle was observed with SEM after an adsorption experiment (initial concentration of 100 mg/L, carbon mass of 50 mg,

Table 7
Parameters of intraparticle diffusion model on GCN816 G

	K_{ID1} (mg/g/$h^{1/2}$)	K_{ID2} (mg/g/$h^{1/2}$)	c_1 (mg/g)	c_2 (mg/g)
40 mg/L–30 mg	2.75	0.92	2.65	15.10
100 mg/L–50 mg	4.29	1.39	2.98	17.82

removal 30 mg/g) in which the final pH resulted to be below the pH value of precipitation for the hydroxide (pH 5.54 was measured by digital pH-meter, against a pH of precipitation theoretically equal to 5.74). Fig. 31 (1,000× enlargement) and Fig. 32 (5,000× enlargement) show that the carbon particle surface appears covered by few solid lead crystals, indicating some presence of precipitate. Precipitation may be explained with the occurrence of phenomena of microprecipitation due to local variation of the pH near the carbon surface. Anyway, the phenomenon appears much less marked with respect to the case of the sample examined in Figs. 29 and 30. In fact, observing Fig. 32 (made with the same enlargement as Fig. 30), access to the internal porosities result clearly visible: if porosities remain accessible to the adsorbate, it is allowed to suppose that the removed lead was effectively adsorbed inside the carbon. This was confirmed by elemental superficial analysis, which showed the lead and oxygen peaks to be very low with respect to the carbon peak. The above comparison analysis confirm that precipitation should be avoided because, even if removal takes place, it obstructs the access to internal porosity thus, limiting the availability of internal adsorption sites for further removal.

3.5.6. Adsorption isotherms of lead

The experimental results concerning the adsorption of lead at equilibrium (96 h) have been interpreted,

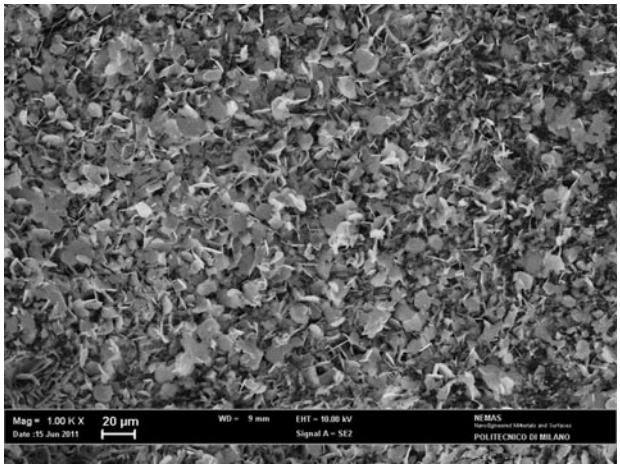

Fig. 29. SEM photograph of lead hydroxide precipitate on GCN816 G (1,000×).

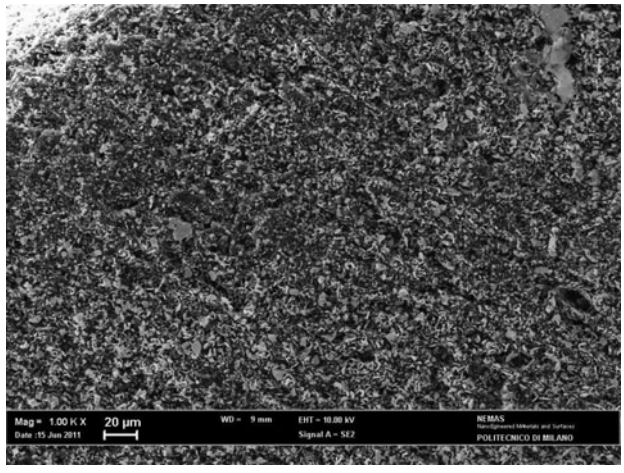

Fig. 31. SEM photograph of lead hydroxide in condition of nonprecipitation on GCN816 G (1,000×).

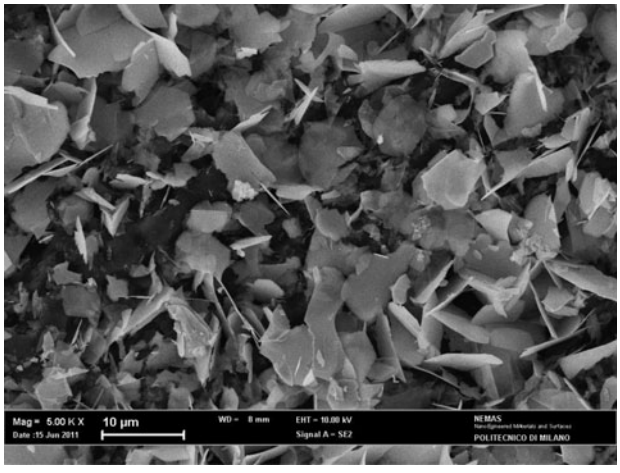

Fig. 30. SEM photograph of lead hydroxide precipitate on GCN816 G (5,000×).

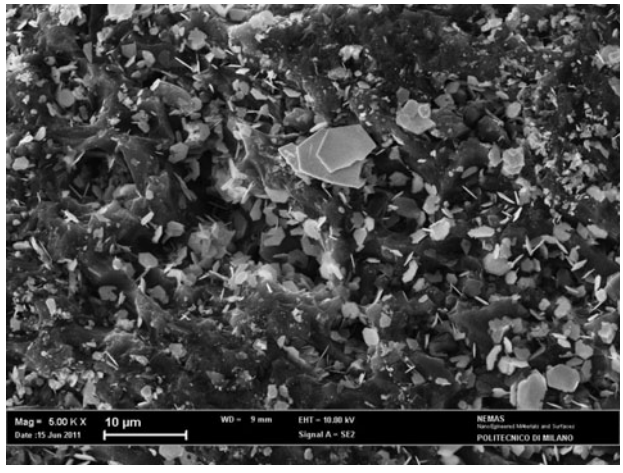

Fig. 32. SEM photograph of lead hydroxide in condition of nonprecipitation on GCN816 G (5,000×).

according to Langmuir and Freundlich adsorption isotherms.

According to the Langmuir model (Eq. (7)), a plot of c_e/q_e vs. c_e resulting in a straight line with a slope of $1/q_{\max}$ and intercept of $1/(q_{\max} \cdot K_L)$, is reported in Fig. 33.

Following the Freundlich model (Eq. (8)), a plot of $\log_{10}(q_e)$ vs. $\log_{10}(c_e)$ was obtained and reported in Fig. 34: it results in a straight line with a slope of $1/n$ and intercept of $\log_{10}(K_F)$.

Fig. 35 allows a comparison among the adsorption isotherm models and the adsorption experimental data. Values of Langmuir and Freundlich constants are shown in Table 8. Experimental data are better interpreted by the Langmuir model ($R^2 = 0.99$) compared to the Freundlich model ($R^2 = 0.75$). As for the GCN816 G activated carbon, the maximum adsorption capacity experimentally found is 32.08 mg/g, which is a value not particularly high but still comparable with other granular activated carbons reported in literature (Table 5).

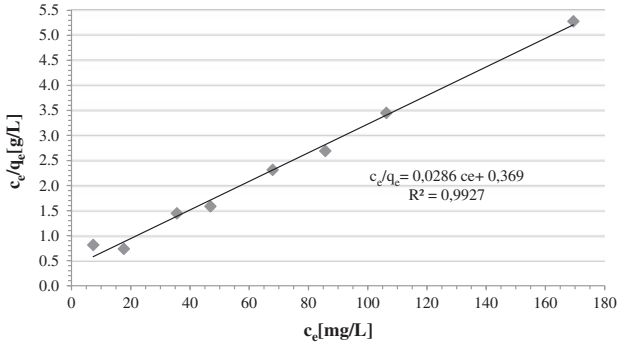

Fig. 33. Langmuir adsorption isotherm of lead on GCN816 G.

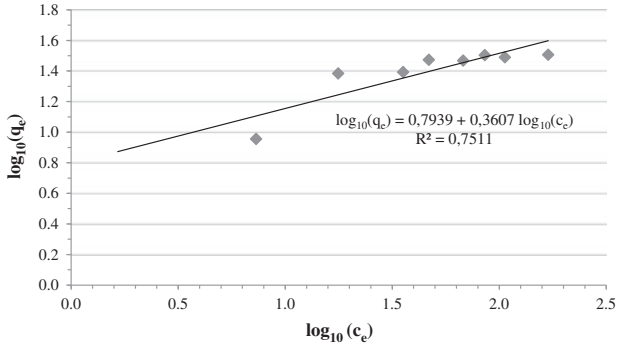

Fig. 34. Freundlich adsorption isotherm of lead on GCN816 G.

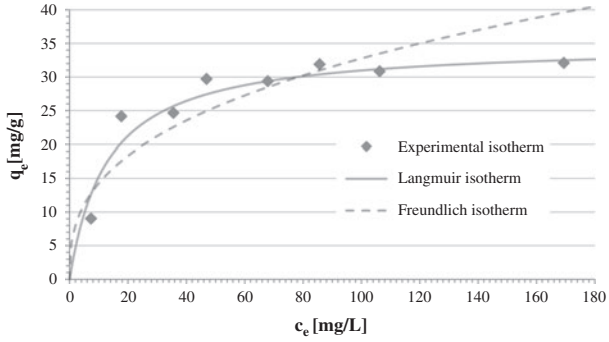

Fig. 35. Lead adsorption isotherms on GCN816 G.

Table 8
Langmuir and Freundlich constants calculated from lead adsorption data on GCN816 G

Langmuir	$q_{\max}$ (mg/g)	K_L (L/mg)	R^2
	34.96	0.078	0.99
Freundlich	*1/n*	K_F [mg/(g (mg/L)$^{1/n}$)]	R^2
	0.36	6.22	0.75

3.5.7. Effect of initial lead concentration on adsorption

The effect of lead concentration was studied using three lead-containing solutions at initial concentrations ranging from 40 to 200 mg/L, at a fixed mass of activated carbon (50 mg). Fig. 36 shows that the removal efficiency of lead decreases as the initial lead concentration increases. This may be due to the fact that, at lower concentrations, the ratio between metal ions and the number of available sites for adsorption is low; as a consequence, the fraction of adsorbed ions becomes independent from the initial concentration. At higher concentrations, available adsorption sites become more rare with respect to the number of ions in solution and so, the efficiency of metal removal depends on initial concentrations [40]. Because of this behavior, considering equal mass of carbon, GCN816 G is more efficient to remove relatively low concentrations of lead, while GCN 1240 is more suitable for highly contaminated solutions.

3.5.8. Effect of carbon mass concentration on adsorption of lead

Removal efficiency vs. carbon mass concentration was obtained by performing equilibrium adsorption experiments at fixed initial lead concentration (100 mg/L) and varying the activated carbon mass in the dispersion (30 mL). Results are plotted in Fig. 37.

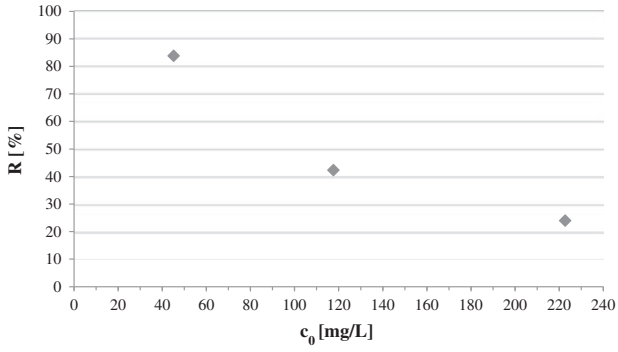

Fig. 36. Effect of initial lead concentration on adsorption on GCN816 G (W = 50 mg).

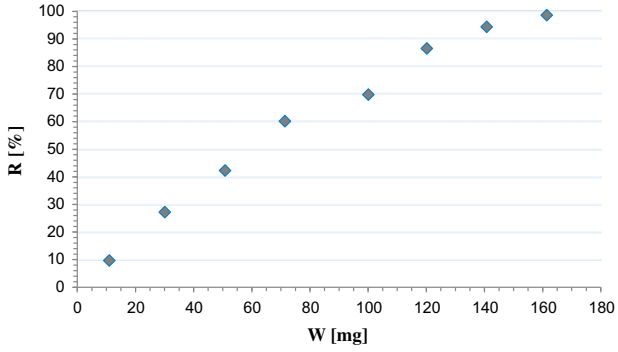

Fig. 37. Effect of carbon mass on lead removal efficiency on GCN816 G (c_0 = 100 mg/L).

Results show that removal efficiency increases if the concentration of activated carbon increases, according to results obtained for GCN1240. A plot of adsorption capacity vs. carbon mass is also reported in Fig. 38: adsorption capacity decreases while carbon concentration increases, suggesting that, at lower carbon concentration, all the active sites are available for metal ions. In particular, the maximum adsorption capacity is reached with 30 mg of carbon into 30 mL of aqueous solution containing 100 mg/L of lead (II). While increasing the activated carbon mass, only a part of the active sites results exposed and occupied by Pb^{2+} ions, justifying a lower adsorption capacity in correspondence of high carbon concentrations [22].

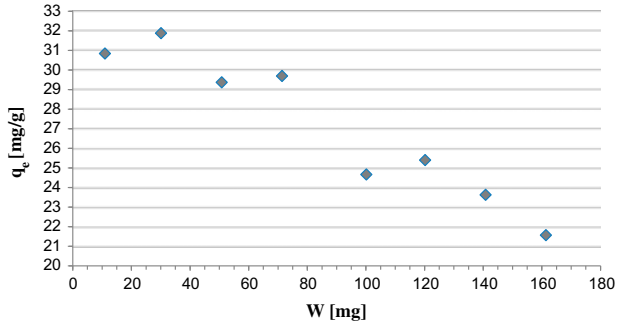

Fig. 38. Effect of carbon mass on lead adsorption capacity on GCN816 G (c_0 = 100 mg/L).

4. Conclusions

The present study was aimed to investigate the feasibility of using, for separation of lead (II) from aqueous solutions, two commercially available granular activated carbons prepared by physical activation of coconut shells selected to purify potable water from dissolved organics (GCN1240) and for use in gold recovery systems (GCN 816 G). The two carbons presented different particle size; a characterization of both the adsorbents was provided through pH_{PZC} measurements and SEM observations. Adsorption tests were conducted in batch laboratory mode. Experimental results discussed in this work lead to the following conclusions:

- both the activated carbons could be successfully used for adsorption of lead (II) ions from aqueous solutions; the maximum adsorption capacity of the studied activated carbons resulted to be 92.39 mg/g (GCN1240) and 32.08 mg/g (GCN 816 G);
- optimal pH value for adsorption in batch laboratory mode was found around 5.0;
- SEM observations showed formations of lead hydroxide crystals on the carbons' surface obstructing the pores at pH values above the pH at which $Pb(OH)_2$ precipitates;
- precipitation should be avoided, because it obstructs the access to internal adsorption sites; to avoid precipitation, due to its alkaline nature, the mass of used carbon should be carefully chosen;
- experimental parameters such as contact time and initial metal concentration must be optimally selected to obtain the highest possible lead removal from the aqueous solution; and
- the very slow kinetics observed with the carbon with bigger particles size allowed to perform a deep investigation about the steps constituting the adsorption mechanism based on the intraparticle diffusion model.

Acknowledgments

The authors gratefully acknowledge the 'Micro and Nanostructured Materials Lab' of NEMAS-Department of Energy—Politecnico di Milano for SEM analyses. Special thanks to M. Giola and A. Mantegazza for their support in the experimental activity.

References

[1] T.G. Chuah, A. Jumasiah, I. Azni, S. Katayon, S.Y.T. Choong, Rice husk as a potentially low-cost biosorbent for heavy metal and dye removal: An overview, Desalination 175 (2005) 305–316.

[2] M. Kobya, E. Demirbas, E. Senturk, M. Ince, Adsorption of heavy metal ions from aqueous solutions by activated carbon prepared from apricot stone, Bioresour. Technol. 96 (2005) 1518–1521.

[3] M. Imamoglu, O. Tekir, Removal of copper (II) and lead (II) ions from aqueous solutions by adsorption on activated carbon from a new precursor hazelnut husks, Desalination 228 (2008) 108–113.

[4] A. Günay, E. Arslankaya, I. Tosun, Lead removal from aqueous solution by natural and pretreated clinoptilolite: Adsorption equilibrium and kinetics, J. Hazard. Mater. 146 (2007) 362–371.

[5] Y. Mido, M. Satake, Chemicals in the Environment, Discovery Publishing House, New Delhi, 1995.

[6] C.K. Singh, J.N. Sahu, K.K. Mahalik, C.R. Mohanty, B. Ray Mohan, B.C. Meikap, Studies on the removal of Pb(II) from wastewater by activated carbon developed from *Tamarind* wood activated with sulphuric acid, J. Hazard. Mater. 153 (2008) 221–228.

[7] B.L. Martins, C.V. Cruz, A.S. Luna, C.A. Henriques, Sorption and desorption of Pb^{2+} ions by dead *Sargassum* sp. biomass, Biochem. Eng. J. 27 (2006) 310–314.

[8] G.W. Goldstein, Neurologic concepts of lead poisoning in children, Pediatr. Ann. 21 (1992) 384–388.

[9] R. Jalali, H. Ghafourian, Y. Asef, S.J. Davarpanah, S. Sepehr, Removal and recovery of lead using nonliving biomass of marine algae, J. Hazard. Mater. 92(3) (2002) 253–262.

[10] M. Gupta, S. Sharma, V.K. Gupta, Process development for the removal of lead and chromium from aqueous solutions using red mud—An aluminium industry waste, Water Res. 35(5) (2001) 1125–1134.

[11] K. Conrad, H.C.B. Hansen, Sorption of zinc and lead on coir, Bioresour. Technol. 98(1) (2007) 89–97.

[12] X. Song, H. Liu, L. Cheng, Y. Qu, Surface modification of coconut-based activated carbon by liquid-phase oxidation and its effects on lead ion adsorption, Desalination 255 (2010) 78–83.

[13] J. Acharya, J.N. Sahu, C.R. Mohanty, B.C. Meikap, Removal of lead(II) from wastewater by activated carbon developed from Tamarind wood by zinc chloride activation, Chem. Eng. J. 149 (2009) 249–262.

[14] J.W. Moore, S. Ramamoorthy, Heavy Metals in Natural Waters: Applied Monitoring and Impact Assessment, Springer, New York, NY, 1984.

[15] USEPA, National Primary Drinking Water Standards, EPA, 2003. Available from: http://www.epa.gov/safewater/consumer/pdf/mcl.pdf.

[16] A. Groffman, S. Peterson, D. Brookins, Removing lead from wastewater using zeolites, Water Environ. Technol. 5 (1992) 54–59.

[17] L. Wang, J. Zhang, R. Zhao, Y. Li, C. Li, C. Zhang, Adsorption of Pb(II) on activated carbon prepared from *Polygonum orientale* Linn.: Kinetics, isotherms, pH, and ionic strength studies, Bioresour. Technol. 101 (2010) 5808–5814.

[18] S.W. Lin, R.M.F. Navarro, An innovative method for removing Hg^{2+} and Pb^{2+} in ppm concentrations from aqueous media, Chemosphere 39(11) (1999) 1809–1817.

[19] D. Petruzzelli, M. Pagano, G. Tiravanti, R. Passino, Lead removal and recovery from battery wastewaters by natural zeolite clinoptilolite, Solvent Extr. Ion Exch. 17(3) (1999) 677–694.

[20] A. Saeed, M. Iqbal, M.W. Akhtar, Removal and recovery of lead(II) from single and multimetal (Cd, Cu, Ni, Zn) solutions by crop milling waste (black gram husk), J. Hazard. Mater. 117(1) (2005) 65–73.

[21] S. Doyurum, A. Çelik, Pb(II) and Cd(II) removal from aqueous solutions by olive cake, J. Hazard. Mater. 138 (1) (2006) 22–28.

[22] Y. Li, Q. Du, X. Wang, P. Zhang, D. Wang, Z. Wang, Y. Xia, Removal of lead from aqueous solution by activated carbon prepared from *Enteromorpha prolifera* by zinc chloride activation, J. Hazard. Mater. 183 (2010) 583–589.

[23] S.J.T. Pollard, G.D. Fowler, C.J. Sollars, R. Perry, Low-cost adsorbents for waste and wastewater treatment: A review, Sci. Total Environ. 116 (1992) 31–52.

[24] I. Ali, V.K. Gupta, Advances in water treatment by adsorption technology, Nat. London 1 (2006) 2661–2667.

[25] I. Ali, The quest for active carbon adsorbent substitutes: Inexpensive adsorbents for toxic metal ions removal from wastewater, Sep. Purif. Rev. 39 (2010) 95–171.

[26] I. Ali, New generation adsorbents for water treatment, Chem. Rev. 112(10) (2012) 5073–5091.

[27] I. Ali, M. Asim, T.A. Khan, Low cost adsorbents for the removal of organic pollutants from wastewater, J. Environ. Manage. 113 (2012) 170–183.

[28] I. Ali, Water treatment by adsorption columns: Evaluation at ground level, Sep. Purif. Rev. 43(3) (2014) 175–205.

[29] J. Goel, K. Kadirvelu, C. Rajagopal, V. Kumar Garg, Removal of lead(II) by adsorption using treated granular activated carbon: Batch and column studies, J. Hazard. Mater. B 125 (2005) 211–220.

[30] M. Sekar, V. Sakthi, S. Rengaraj, Kinetics and equilibrium adsorption study of lead(II) onto activated carbon prepared from coconut shell, J. Colloid Interface Sci. 279(2) (2004) 307–313.

[31] C.P. Dwivedi, J.N. Sahu, C.R. Mohanty, B. Raj Mohan, B.C. Meikap, Column performance of granular activated carbon packed bed for Pb(II) removal, J. Hazard. Mater. 156(1–3) (2008) 596–603.

[32] W. Su, L. Zhou, Y. Zhou, Preparation of microporous activated carbon from coconut shells without activating agents, Carbon 41(4) (2003) 861–863.

[33] C.J. Kirubakaran, K. Krishnaiah, S.K. Seshadri, Experimental study of the production of activated carbon from coconut shells in a fluidized bed reactor, Ind. Eng. Chem. Res. 30(11) (1991) 2411–2416.

[34] X. Tao, L. Xiaoqin, Peanut shell activated carbon: Characterization, surface modification and adsorption of Pb^{2+} from aqueous solution, Chin. J. Chem. Eng. 16 (3) (2008) 401–406.
[35] K. Wilson, H. Yang, C.W. Seo, W.E. Marshall, Select metal adsorption by activated carbon made from peanut shells, Bioresour. Technol. 97 (2006) 2266–2270.
[36] J.W. Kim, M.H. Sohn, Production of granular activated carbon from waste walnut shell and its adsorption characteristics for Cu^{2+} ion, J. Hazard. Mater. 85 (2001) 301–315.
[37] G. Issabayeva, M.K. Aroua, N.M.N. Sulaiman, Removal of lead from aqueous solutions on palm shell activated carbon, Bioresour. Technol. 97(18) (2006) 2350–2355.
[38] M.M. Johns, W.E. Marshall, C.A. Toles, Agricultural by-products as granular activated carbons for adsorbing dissolved metals and organics, J. Chem. Technol. Biotechnol. 71(2) (1998) 131–140.
[39] K. Zhang, W.H. Cheung, M. Valix, Roles of physical and chemical properties of activated carbon in the adsorption of lead ions, Chemosphere 60(8) (2005) 1129–1140.
[40] M.M. Rao, G.P. Rao, K. Seshaiah, N.V. Choudary, M.C. Wang, Activated carbon from *Ceiba pentandra* hulls, an agricultural waste, as an adsorbent in the removal of lead and zinc from aqueous solutions, Waste Manage. 28(5) (2008) 849–858.
[41] Z. Li, X. Tang, Y. Chen, L. Wei, Y. Wang, Activation of *Firmiana simplex* leaf and the enhanced Pb(II) adsorption performance: Equilibrium and kinetic studies, J. Hazard. Mater. 169(1–3) (2009) 386–394.
[42] P. Shekinah, K. Kadirvelu, P. Kanmani, P. Senthilkumar, V. Subburam, Adsorption of lead(II) from aqueous solution by activated carbon prepared from *Eichhornia*, J. Chem. Technol. Biotechnol. 77(4) (2002) 458–464.
[43] R. Balasubramanian, S.V. Perumal, K. Vijayaraghavan, Equilibrium isotherm studies for the multicomponent adsorption of lead, zinc and cadmium onto indonesian peat, Ind. Eng. Chem. Res. 48(4) (2009) 2093–2099.
[44] Y.S. Ho, G. McKay, Pseudo-second order model for sorption processes, Process Biochem. 34(5) (1999) 451–465.
[45] Y. Qiu, H. Cheng, C. Xu, D. Sheng, Surface characteristics of crop-residue-derived black carbon and lead (II) adsorption, Water Res. 42(3) (2008) 567–574.
[46] V.V. Simonova, L.N. Isaeva, Y.V. Tamarkina, T.G. Shendrik, V.A. Kucherenco, Lead adsorption on brown coal activated with potassium hydroxide, Solid Fuel Chem. 44(2) (2009) 109–111.
[47] M.K.B. Gratuito, T. Panyathanmaporn, R.A. Chumnanklang, N. Sirinuntawittaya, A. Dutta, Production of activated carbon from coconut shell: Optimization using response surface methodology, Bioresour. Technol. 99(11) (2008) 4887–4895.
[48] B. Volesky, Biosorption of Heavy Metal, CRC Press, Boston, MA, 1990.
[49] C.F. Baes Jr., R.E. Mesmer, The Hydrolysis of Cations, Wiley, New York, NY, 1976.
[50] M.V. Lopez-Ramon, F. Stoeckli, C. Moreno-Castilla, F. Carrasco-Marin, On the characterization of acidic and basic surface sites on carbons by various techniques, Carbon 37(8) (1999) 1215–1221.
[51] M. Mullet, P. Fievet, A. Szymczyk, A. Foissy, J.C. Reggiani, J. Pagetti, A simple and accurate determination of the point of zero charge of ceramic membranes, Desalination 121(1) (1999) 41–48.
[52] S. Brunauer, P.H. Emmett, E. Teller, Adsorption of gases in multimolecular layers, J. Am. Chem. Soc. 60 (2) (1938) 309–319.
[53] M. Caccin, F. Giacobbo, M. Da Ros, L. Besozzi, M. Mariani, Adsorption of uranium, cesium and strontium onto coconut shell activated carbon. J. Radioanal. Nucl. Chem. 297(1) (2013) 9–18.
[54] P. Patnukao, A. Kongsuwan, P. Pavasant, Batch studies of adsorption of copper and lead on activated carbon from *Eucalyptus camaldulensis* Dehn. bark, J. Environ. Sci. 20 (2008) 1028–1034.
[55] M.A. Ferro-García, J. Rivera-Utrilla, I. Bautista-Toledo, Removal of lead from water by activated carbons, Carbon 28(4) (1990) 545–552.
[56] S.Z. Mohammadi, M.A. Karimi, D. Afzali, F. Mansouri, Removal of Lead (II) from aqueous solutions using activated carbon from Sea-buckthorn stones by chemical activation, Desalination 262(1–3) (2010) 86–93.
[57] H. Cho, D. Oh, K. Kim, A study on removal characteristics of heavy metals from aqueous solution by fly ash, J. Hazard. Mater. B 127(1–3) (2005) 187–195.
[58] B. Yu, Y. Zhang, A. Shukla, S.S. Shukla, K.L. Dorris, The removal of heavy metals from aqueous solutions by sawdust adsorption—Removal of lead and comparison of its adsorption with copper, J. Hazard. Mater. B 84 (2001) 83–94.